AMERICAN ACADEMY OF OPHTHALMOLOGY®

Advanced Optical Analysis of Divergence Between the Foci of the Neodymium-Doped Yttrium Aluminum Garnet (Nd:YAG) and Aiming Beam Lasers

Edward Averbukh, MD,[1,*] *Yaakov Slushetz, MSc,*[2,*] *Jaime Levy, MD,*[1] *Rani Patal, MD,*[1] *Yaakov Mandelbaum, PhD,*[2] *Yoel Arieli, PhD*[2]

Purpose: To evaluate the divergence between the neodymium-doped yttrium aluminum garnet (Nd:YAG) surgical laser and the aiming diode laser beams foci.

Design: Optical analysis and measurements were performed using a Volk Goldmann 3-mirror lens with a Nidek YC-1800 Nd:YAG laser apparatus.

Subjects: None.

Methods: We used the Zemax OpticStudio program for the model of Nd:YAG treatment in a human eye. Additionally, theoretical calculations were performed.

Main Outcome Measures: The divergence between the Nd:YAG laser focus and the intersection of the 2 aiming beams inside the eye.

Results: Focal points of the 2 laser beams converge 8 mm behind the cornea. Posterior to this point, the intersection of the diode laser aiming beams lies in front of the focal point of the Nd:YAG treatment laser, with distance between the 2 foci progressively increasing up to 305 microns at 24 mm behind the cornea.

Conclusions: We report the degree of divergence between the 2 lasers' focal points due to the difference in refraction between the corresponding wavelengths. These results have high practical relevance, as they provide a starting point for increasing the accuracy of Nd:YAG laser treatment, particularly when applied to the posterior segment, thereby minimizing the risk of complications. Current Nd:YAG laser devices have the built-in ability to modify the focal point of the aiming beam along the *z*-axis, thus providing possibility for an immediate application of our findings in clinical practice.

Financial Disclosures: The authors have no proprietary or commercial interest in any materials discussed in this article. *Ophthalmology Science 2024;4:100512 © 2024 by the American Academy of Ophthalmology. This is an open access article under the CC BY-NC-ND license (http://creativecommons.org/licenses/by-nc-nd/4.0/).*

Supplemental material available at www.ophthalmologyscience.org.

Neodymium-doped yttrium aluminum garnet (Nd:YAG) is a synthetic crystal used in solid-state lasers. One of the main advantages of an Nd:YAG laser is that in its Q-switched mode it can deliver pulsed energy that causes photodisruption, rather than coagulating the tissue. In practice, this means that the energy delivered to the target tissue produces plasma, vapor bubbles, and an acoustic shock wave that ruptures the tissue at the laser's focal point. In 1973, Beckman and Sugar first reported the use of an Nd:YAG laser for cyclodestruction in ophthalmology.[1]

The wavelength of light emitted by an Nd:YAG crystal lies in the invisible infrared spectrum. Therefore, to visualize the predicted focal point of the Nd:YAG laser beam, a second red, visible laser is aligned with and used to aim the Nd:YAG laser. At a spatial point where the 2 aiming beams converge into 1, the practitioner will know that this is the location where the energy of the treatment beam is concentrated.[2,3]

Typically, Nd:YAG laser machines use a cone-shaped laser beam with 2 aiming beams outlining the Nd:YAG laser cone.[4] This cone configuration allows the unfocused energy to pass through transparent tissues without causing any damage, while creating the desired disruptive effect in the target tissue deep inside the eye. The ability to cut tissues inside the eye while keeping the eye-wall intact is the most valuable advantage of this type of laser. However, as it passes through different tissues deep in the eye, the light is refracted, and different wavelengths are refracted differently, a phenomenon known as chromatic aberration. As a result, the focal points of the diode and Nd:YAG lasers may not be aligned precisely. Ophthalmic surgical lasers therefore have the added ability to adjust the focus along the z-axis (anteriorly or posteriorly) to compensate for this aberration.

In clinic, we use the ability of Nd:YAG machine foci adjustment in daily practice for anterior segment procedures.

https://doi.org/10.1016/j.xops.2024.100512
ISSN 2666-9145/24

The manual, and our personal experience with the machine, both indicate that the offset may be changed by up to 500 microns in either direction using steps of 25 microns.[5] Proper use of this feature assumes that the location of the treatment beam's focal point, indicated by the device control, is correct. However, within the eye, refraction by the tissue causes a shift in the focal point location. The aiming beam intersection point is shifted as well, yet due to intraocular dispersion, the shifts are not equal. The device's control dial thus loses its calibration. The purpose of this study is to quantify the disparity in the 2 shifts and thus restore the ability to calibrate the instrument readout of the focal point location.

This modulation of the offset makes our results applicable immediately to any similar machine, improving the efficacy and safety of any laser-assisted procedure performed in the posterior pole.

Methods

For this study, we used a Nidek YC-1800 laser machine. It has a Q-switched Nd:YAG laser beam (1064 nm wavelength) for treatment and 2 diode laser beams (635 nm wavelength) for aiming. The diode beams intersect and are focused at the same point.

Measurement of the Aiming-Beam Intersection Angle

The angle of intersection of the aiming beams was measured by observing their transillumination on a 5mm grid paper, placed in the plane of the rays. Based on this, the half-angle value used subsequently in the analysis was 8°. (For further detail, see the "Technical Details" section in the Supplementary Data.)

Modeling the Rays by Software

To model the divergence along the z-axis between the 2 lasers' focal points, a light-cone of angle 16° (half-angle equal to 8°) and wavelength 1064 nm was created in the existing eye model in the Zemax OpticStudio (ZOS), together with a pair of rays of wavelength 635 nm, that cross and focus at the same point. The mechanical displacement between the 2 beam systems was assumed fixed such that in air (zero dispersion) there is no deviation and the foci coincide.

The first-order equation of chromatic aberration is given by the (first-order) differential of the focal distance with respect to changes in the wavelength.

Let Δn be the variation in the refractive index due to the range of wavelengths $\Delta\lambda$,

$$\Delta n \cong \frac{dn}{d\lambda}\Delta\lambda.$$

Then the first-order equation of the chromatic aberration Δf is:

$$\Delta f = \frac{df}{dn}\Delta n$$

where f is the focal length, and n is the refractive index at a specific point in the medium. This equation can be used to calculate the chromatic aberration for different wavelengths in the spectrum or different locations within the eye.

Quantitative Description

Refraction of the light in the eye can be quantified using the refractive index, n. To calculate the focal point of a beam passing through a surface within a medium, Gauss's formula is used.

In the given context, the incident parallel beam is described as coming from infinity, as it is approximately parallel to the optical axis. From this, it follows that Gauss's formula takes the form

$$\frac{n'}{s'_\infty} = \frac{1}{f}$$

and it can be seen that the focal point, located at a distance $s'_\infty = n'f$, depends on the refractive index of the medium through which the beam passes.

The chromatic longitudinal aberration refers to the color distortion along the optical axis across the visible spectrum and is calculated depending on the focal length of the lens. The basic formula for calculating the expected aberration calculates the difference between the focal points of different wavelengths.

In simplified form, it appears as

$$\mathrm{CLA} = \Delta f_{\mathrm{Vis.}} = \frac{df}{dn}\Delta n_{\mathrm{Vis.}} = \frac{f}{V},$$

with $\Delta n_{\mathrm{Vis.}}$ and $\Delta f_{\mathrm{Vis.}}$ the variation of the refractive index and the focal length, respectively, across the visible spectrum. The "Abbe Number," V, is defined by the formula

$$V = \frac{n_{\mathrm{d}} - 1}{n_{\mathrm{C}} - n_{\mathrm{F}}}$$

where n_{F} is the refractive index at the short wavelength (blue), n_{C} is the refractive index at the long wavelength (red), and n_{d} is the refractive index at the middle wavelength (yellow).

In our case, we evaluate the chromatic aberration due to the difference in wavelength between the Nd:YAG beam at 1064 nm, and the red guide-beams (aiming beams) at 635 nm, rather than the aberration across the visible range.

The expression for the chromatic longitudinal aberration can be adapted by rescaling the visible-range aberration by the factor. $\frac{\Delta\lambda_{\mathrm{Guide-YAG}}}{\Delta\lambda_{\mathrm{Vis.}}}$ where $\Delta\lambda_{\mathrm{Vis.}} \equiv \lambda_{\mathrm{C}} - \lambda_{\mathrm{F}}$ and $\Delta\lambda_{\mathrm{Guide-YAG}} \equiv \lambda_{\mathrm{Nd:YAG}} - \lambda_{\mathrm{Guide}}$ ..

This can be written:

$$\Delta f_{\mathrm{Guide-YAG}} = \frac{f}{\tilde{V}},$$

using a rescaled Abbe number,

$$\tilde{V} \equiv V\frac{\Delta\lambda_{\mathrm{Vis.}}}{\Delta\lambda_{\mathrm{Guide-YAG}}}.$$

However, the formula becomes more complex when dealing with thick lenses, when the material on either side of the lens is not air, or when the incoming beam is not collimated. Here, we present the formulas that can be used in the eye, which has multiple surfaces and refractive indices (the complete development is presented in the section "Technical Details" section in the Supplementary Data).

The chromatic aberration is the deviation $\Delta s'$ between the focal distance (intersection), distance of the red aiming beams, and the focal point of the Nd:YAG light-cone, which satisfies

$$\Delta s' = \left(n_{\mathrm{V}}\frac{\Delta\Omega}{\Omega + \frac{n}{s}} - \frac{n_{\mathrm{V}} - 1}{\tilde{V}_{\mathrm{V}}}\right)\frac{1}{\Omega + \frac{n}{s}} = \left(\frac{\Delta\Omega}{\Omega + \frac{n}{s}} - \frac{1 - \frac{1}{n_{\mathrm{V}}}}{\tilde{V}_{\mathrm{V}}}\right)s' = \left(\frac{\Delta\Omega}{n_{\mathrm{V}}}s' - \frac{1 - \frac{1}{n_{\mathrm{V}}}}{\tilde{V}_{\mathrm{V}}}\right)s'$$

where the subscript "V" denotes the vitreous humor, and

$$\Omega \equiv \frac{1}{f}$$

The latter is known as the "optical power;" the depth of the focal point within the eye, s' can be computed from the location of the focal point s' before entering the eye (via the Gauss formula) as

$$s' = \frac{n'}{\Omega + \frac{n}{s}},$$

For thin lenses, the total power is given by:

$$\Omega = \Omega_1 + \Omega_2 + \ldots + \Omega_n,$$

where it follows from above that the power of each surface is given by

$$\Omega_i = \frac{n_{i+1} - n_i}{R_{i+1}},$$

The total chromatic deviation in the power $\Delta\Omega$ is expressed as the sum of the aberrations for each surface:

$$\Delta\Omega = \Delta\Omega_1 + \Delta\Omega_2 + \ldots + \Delta\Omega_n$$

Finally, the aberration for a beam passing from refractive index n_i to refractive index n_{i+1} is calculated using $\frac{1}{\tilde{V}_i}$:

$$\begin{aligned}\Delta\Omega_i &= \left(\frac{n_{i+1}-1}{\tilde{V}_{i+1}} - \frac{n_i - 1}{\tilde{V}_i}\right)\frac{\Omega_i}{n_{i+1} - n_i} \\ &= \left(\frac{n_{i+1}-1}{\tilde{V}_{i+1}} - \frac{n_i - 1}{\tilde{V}_i}\right)\frac{1}{R_{i+1}}.\end{aligned}$$

By substituting the values of the parameters − index of refraction, n_i, curvature, R_i, and (adjusted) Abbe number, $\tilde{V}_i$ of the tissues in the eye, the following first-order model was obtained for the deviation between the Nd:YAG-beam focus and the aiming-beam intersection as a function of the depth of the latter within the eye:

$$\begin{aligned}\Delta\mathbf{s}' &= \left(\frac{\Delta\Omega}{\mathbf{n_V}}\mathbf{s}' - \frac{1 - \frac{1}{\mathbf{n_V}}}{\tilde{\mathbf{V}}_\mathbf{V}}\right)\mathbf{s}' = \left(\frac{3.278}{1.34}\mathbf{s}' - \frac{1 - \frac{1}{1.34}}{21.17}\right)\mathbf{s}' \\ &= \mathbf{2.446s'^2 - 0.012s'}\end{aligned}$$

Measuring the Focal Length of an Ophthalmic Lens

Given the fact that the emmetropic eye's structure (the model eye) causes convergence of parallel light rays on the retina, any beam of light that is already convergent, like the Nd:YAG laser, cannot be focused on the retina; the maximal depth of its focus inside the eye will be just behind the lens. A diverging lens that cancels the eye's converging effect is needed to focus this laser on the posterior pole of the eye and perform treatments in this region. In our model, we simulated the use of a Volk Goldmann 3-mirror lens, as reported by Mainster,[5] to focus the laser beam on the posterior pole of the eye. For theoretical measurements and modeling, we used the ZOS Simulation software program[6] (Radiant ZOS LLC) that emulates refraction by computer modeling. This system allowed us to measure the optical aberrations arising from the different wavelengths, based on the geometry of our model.[7–9]

In this study, we used 3 methods to determine the dioptric power of the lenses and their focal points. First, we used the traditional method of measuring the parameters of the real image in the distance, for example by projecting the light on a screen. This method is suitable only for converging lenses; to measure a diverging lens, a converging lens with a known higher absolute dioptric power is aligned with the diverging lens during the measurements. The power of the diverging lens is calculated by subtracting the known power of the converging lens from the result.

This traditional method is less suitable for submillimeter precision. We therefore also measured the lens using a Melos measuring system obtained from Möller−Wedel[10] in which a direct beam passing through the lens forms the image in the focal plane. To determine the focal point of the lens, the image should be in focus. The upper part of the device is a glass table with calibration scales that are used to measure the exact size of the image. Following a 1-time calibration method,[11] the size of the image can be used to determine the focal length.

Measurements of the focal length were also performed using approximately monochromatic sources of several wavelengths. The measurements were carried out using an infinity-corrected system. This method is similar to auto-collimation. However, instead of using a mirror, an additional focusing lens is placed in the path of the reflected light, and the image is obtained on a screen or paper at the focal point. The Melos device is also based on an infinity-corrected optical system. With the method used, however, when measuring a plano-concave lens of nonnegligible thickness such as the Volk Goldmann, both the index of refraction and the radius of curvature are determined. In this case, the former was found to be about $n = \frac{2.7}{1.5} = 1.8$, and the latter approximately $R = \frac{EFL}{n-1} = \frac{-2cm}{0.8} = -2.5$ cm.

It is important to note that the digital lensometers commonly used to measure the power of eyeglasses were not suitable for our study, as the dioptric power of the diverging lenses used for laser treatments far exceeds the range of these instruments. However, using the focal points of the lenses in air, it is possible to calculate the difference in focal points between the diode laser beam and the Nd:YAG laser beam after they pass through the refractive media—the cornea, the lens, and the vitreous. We present these data both graphically and in a table, as a function of depth of the 2 aiming beams intersection in the eye.

Measurements were made at each of the 3 wavelengths: red, blue, and green. The spectra of the light sources[11] used in the measurements can be found in the Technical Details online-only appendix.

Chromatic Aberration Measurement—Extrapolation to Near-Infrared

This work showed that the focal length of the lens is not dependent on the measured wavelength, suggesting that the ophthalmic lens (Volk 3-mirror lens) is optimally designed to minimize chromatic aberration, at least in visible light. The extent of deviation in the near-infrared can be estimated by considering the refractive index as a function of wavelength for BK-7, a common optical glass (see Fig. 3 in the article by Slushetz et al[11]).

As the wavelength increases, the refractive index decreases, and in particular flattens out. At large wavelengths, the refractive index converges monotonically toward an asymptotic value n_∞. According to the lensmaker's equation, the focal length of a plano-concave lens, $\frac{1}{R_1} = 0$, is given by:

$$f = \frac{n-1}{R_2}$$

Clearly there exists an inverse relationship between the focal length of the lens and its refractive index. Thus the focal length of the lens will increase and converge monotonically to an asymptotic value. As long as $n_\infty - 1 \neq 0$, the latter will be finite and the curve will

again flatten out (see Fig. 3 and Table 1 in the article by Slushetz et al[11]). The difference in focal length of this lens for the red aiming beam wavelength and the YAG wavelength, is about the same or smaller than the focal deviation in the visible range:

$$\Delta f_{\text{Guide}-\text{YAG}} \lesssim \text{CLA}$$

In conclusion, since the measurements of the focal length for the Goldmann 3-mirror lens conducted at (3) shorter, visible wavelengths found similar results for all of them, the chromatic aberration will not cause any significant separation of foci between the aiming beam and the Nd:YAG beam within the lens and it can be assumed to be negligible.

Results

Here, we analyzed the divergence predicted to occur between the focal points of the Diode beam and the Nd:YAG beam (used for aiming and treatment, respectively) along the z-axis. When adding the diverging lens to the model, it is imperative to define both its power and focal point. One of the common lenses that allows a direct (noninverted) view of the fundus is the Goldmann-type 3-mirror lens (its central part). The power of such lens may vary slightly between different manufacturers.[12,13] For this study, we used a Volk lens with a power of $\Omega = -67$ diopters.

We describe the progressive divergence between the focal points of the 2 laser beams in our theoretical model by repeatedly calculating it at different distances of the laser from the eye. The closer the laser machine is to the eye, the deeper its foci become inside the eye. The results are presented in Table 1 and graphically in Figure 1.

A best-fit quadratic approximation was obtained to describe the graph:

Figure 1. The graph shows the distance between the 2 focal points, neodymium-doped yttrium aluminum garnet (Nd:YAG) and its aiming beam, as a function of the depth inside the eye. As the device is moved closer to the eye, the depth of the focal points of both the Nd:YAG and of diode laser increases, while the 2 points progressively diverge from one another.

$$\Delta s' = \mathbf{0.8536}s'^{\mathbf{2}} - \mathbf{7.5733}s' + \mathbf{6.0183}$$

Table 1 and Figure 1 show the predicted distance between the 2 focal points as a function of the depth inside the eye. Figure 2 shows how the analytical model compares to ZOS calculation.

We found that the predicted distance between the focal points (f_{YAG}-f_{Guide}) changes from a negative value to a positive value approximately 8 mm inside the eye, as the laser is moved closer to eye. Anterior to this convergence

Table 1. Separation Between the Nd:YAG and Diode Laser Foci as a Function of Depth Within Eye

Distance to Eye (mm)	Depth Within Eye (mm)	Separation (Micron)
28.58	7.42	−3.35
28.00	8.00	−0.03
27.50	8.50	3.28
27.00	9.00	7.01
26.00	10.00	15.73
25.00	11.00	26.12
24.00	12.00	38.19
23.00	13.00	51.94
22.00	14.00	67.38
21.00	15.00	84.52
20.00	16.00	103.35
19.00	17.00	123.89
18.00	18.00	146.14
17.00	19.00	170.11
16.00	20.00	195.82
15.00	21.00	223.27
14.00	22.00	252.47
13.00	23.00	283.45
12.33	23.67	305.22

As we move the machine closer to eye, the foci are getting deeper and the separation grows. Nd:YAG = neodymium-doped yttrium aluminum garnet.

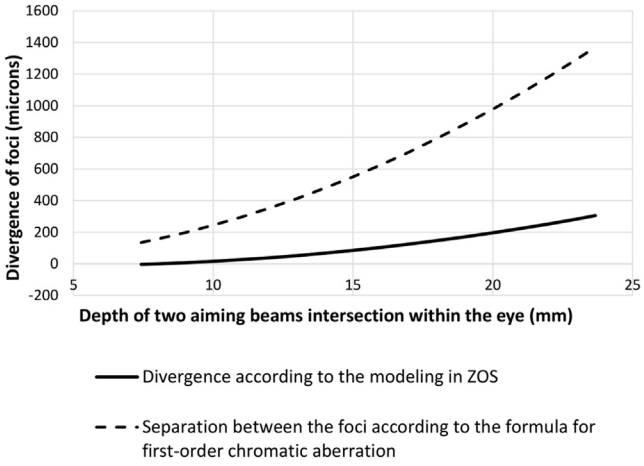

Figure 2. Divergence between foci of neodymium-doped yttrium aluminum garnet and aiming beam as a function of the depth inside the eye. Analytical calculation using first-order aberrations as compared to modeling in Zemax OpticStudio (ZOS). The analytical model is shown in the dashed line while the ZOS model is represented by a solid line. One can see that both models show increased separation of foci with deeper aiming. The analytical model, however, does not account for lens thickness, but rather assumes that all lenses are ideal and thin; thus, it is overestimating the divergence between foci.

point, the focal point of the Nd:YAG laser lies in front of the focal point of the diode aiming beam; posterior to this point, the focal point of the Nd:YAG laser lies behind the focal point of the diode aiming beam.[11] When the thin rays strike the surface of the eye orthogonally, they undergo no dispersion; consequently, the chromatic aberration is zero.[11]

Discussion

In this work we have considered the influence of intraocular dispersion. We calculated the divergence between focal points of an Nd:YAG laser beam and a diode laser beam using a Nidek Nd:YAG laser device with a Volk Goldmann-type 3-mirror lens. For this purpose, we relied on Zemax optical software, which accounted for the dispersion in ocular tissues. According to the calculation, the foci diverge, reaching 305.3 microns at a distance of 24 mm behind the cornea. While the results themselves are not unexpected, it is important to note that the manufacturer does not provide these data, nor have they been published previously in a peer-reviewed article. Indeed, our motivation for conducting this study was the general paucity of relevant data.

An analytical model was developed for use alongside the numerical calculation performed by ZOS. It can be observed that both the graph obtained from the analytical calculation and the graph obtained from ZOS software bear the same general form. The discrepancy between them arises from the fact that the eye cannot be considered a thin lens, which is an assumption of the analytical model.

Neodymium-doped yttrium aluminum garnet lasers are currently used in ophthalmology for a variety of procedures, including iridotomy, pupilloplasty, synechiolysis, anterior and posterior capsulotomy, and vitreolysis.[6] Their cone-shaped beam allows the light energy to pass through the cornea without causing damage while producing the desired therapeutic photodisruption inside the eye. Complications associated with the use of an Nd:YAG laser include retinal breaks, retinal detachment, and damage to lens.[14–16] Some of these complications, such as laser-induced pitting of the intraocular lens (IOL), might be the direct result of incorrect modulation of the target along the z-axis.[16]

The importance of accuracy while aiming the laser beam cannot be overemphasized.

While focusing on a target in the x-y plane is relatively straightforward,[4] focusing along the z-axis is considerably more difficult due to the above-mentioned chromatic aberrations. Moreover, since the early applications of Nd:YAG laser in ophthalmology were designed to treat pathologies in the anterior segment, calibration of the Nd:YAG laser machines using the diode laser was initially optimized for the anterior segment.

In recent years, however, there has been a trend toward using this laser in the posterior segment for procedures such as vitreolysis aimed at vitreous floaters,[17] decompression of the posterior hyaloid to remove trapped blood,[18–20] and dislodging central arterial emboli.[21] Given the proximity of the retina, even a small deviation along the z-axis can cause severe damage, leading to complications such as bleeding, retinal breaks, retinal detachment, and macular holes.[22,23] We realized that there is a need to quantify the degree of divergence between the 2 laser beams when targeting the posterior segment. To address this issue, we modeled the divergence between the focal points of Nd:YAG and diode laser beams over distance.

Dispersion of the Volk lens itself was not considered, as no significant dispersion was detected when this was measured. Therefore, an ideal (paraxial) lens was employed as our initial model. Effectively, this implement made the assumption that the lens was designed to operate in the visible range and at 1064 nm, and that it was tailored to show no aberration between these 2 wavelengths. The effect of deviations from this assumption will be investigated in further efforts.

Nearly 3 decades ago, Tsai et al[24] described their procedure for performing vitreolysis in which they focused the laser on the retina and then gradually retracted it until it was focused on the floater. However, neither they nor others mention any compensation for the expected chromatic aberration.[25] When teaching ophthalmology residents to perform laser posterior capsulotomy, we routinely instruct them to position the Nd:YAG beam 150−250 microns posterior to the visible target of the diode laser to avoid pitting of the IOL; this instruction is based largely on our knowledge and experience, not on any theoretical calculation. However, when dealing with subhyaloid hemorrhage and floaters located adjacent to the retina, it became clear to us that we lack sufficient experience and are unwilling to take any unnecessary risks that may cause complications significantly more severe than pitting of the IOL.[25,26] Indeed, our results show that to align both focal points 24 mm behind the cornea, in our setting one should position the focal point of the Nd:YAG laser beam 305 microns anterior to the focal points (and crossing point) of the visible diode laser beams. This adjustment, which is accomplished relatively easily, will likely increase safety and efficacy when using an Nd:YAG laser to treat lesions close to the retinal plane. For floaterectomy, measuring the position of floaters inside the eye by ultrasound or by OCT might be important to further improve the precision of treatment. The Nidek YC-1800 can adjust the offset up to ±500 microns in 25-micron steps[5] allowing for immediate implementation of our findings.

A limitation of our study is that we evaluated only a single laser device and a single lens; we did not study the more modern lenses that were designed specifically to treat the vitreous pathologies such as the Ocular Karickhoff lens, Ocular Peyman lens, or Volk Singh lens. However, the basic principles behind the chromatic aberrations and our modeling of it should apply to any direct-view lens, and the Goldmann 3-miror lens is still used and readily available in most ophthalmic clinics. Another limitation of our study is the lack of clinical or even laboratory experience that might differ from theoretical calculations; a clinical study, however, will necessitate an entirely different setting. We are aware that the results might differ in pseudophakic eyes; however, any modification of the existing ZOS software model of the human eye to account for pseudophakia will

necessitate multiple calculations for a plethora of different IOLs in clinical use. This project has yet to be attempted exhaustively; it is currently under consideration as an avenue of further investigation, with clear applications.

In summary, the 1064-nm wavelength Nd:YAG laser beam refracts less than the 635-nm wavelength diode laser beam, resulting in a deeper focus for the Nd:YAG laser, if this difference is not accounted for and corrected optically. In our setting, this distance was 305 microns. We have neither ambition nor means to calculate this number for all the Nd:YAG laser machines on the market. We therefore encourage manufacturers of laser devices for ophthalmic procedures to provide the relevant data regarding their devices, and we recommend that clinicians exercise caution when treating posterior segment pathologies using an Nd:YAG laser.[27]

Footnotes and Disclosures

Originally received: May 3, 2023.
Final revision: February 11, 2024.
Accepted: March 8, 2024.
Available online: March 16, 2024. Manuscript no. XOPS-D-23-00088.

[1] Faculty of Medicine, Department of Ophthalmology, Hadassah University Medical Center, Hebrew University, Jerusalem, Israel.

[2] Department of Electro-Optics, Jerusalem College of Technology, Jerusalem, Israel.

*Equal contribution.

Disclosure(s):

All authors have completed and submitted the ICMJE disclosures form.

The author(s) have made the following disclosure(s):

J. L.: Honoraria; Treasurer − Israeli Society for Vision and Eye Research (ISVER).

HUMAN SUBJECTS: No human subjects were included in this study.

No animal subjects were used in this study.

Author Contributions:

Conception and design: Averbukh, Slushetz, Levy, Patal, Mandelbaum, Arieli

Data collection: Averbukh, Slushetz, Mandelbaum, Arieli

Analysis and interpretation: Averbukh, Slushetz, Levy, Patal, Mandelbaum, Arieli

Obtained funding: N/A

Overall responsibility: Averbukh, Slushetz, Levy, Patal, Mandelbaum, Arieli

Abbreviations and acronyms:
IOL = intraocular lens; **Nd:YAG** = neodymium-doped yttrium aluminum garnet; **ZOS** = Zemax OpticStudio.

Keywords:
Optical analysis, Nd:YAG laser, Vitreolysis, Floaterectomy.

Correspondence:
Edward Averbukh, MD, Department of Ophthalmology, Hadassah Medical Center, P.O. Box 12000, Jerusalem 91120, Israel. E-mail: edward@hadassah.org.il.

References

1. Beckman H, Sugar HS. Neodymium laser cyclocoagulation. *Arch Ophthalmol*. 1973;90:27−28.
2. Fankhauser F, Kwasniewska S. *Lasers in Ophthalmology: Basic, Diagnostic, and Surgical Aspects : A Review*. Amsterdam, The Netherlands: Kugler Publications; 2003:304.
3. L'Esperance FA. *Ophthalmic Lasers*. St Louis, MO: Mosby; 1989.
4. Rol P, Fankhauser F, Kwasniewska S. Aiming accuracy in ophthalmic laser microsurgery. *Ophthalmic Surg*. 1986;17:278−282.
5. Ophthalmic YAG laser system YC-1800. Aichi, Japan: Nidek. https://go2.nidek.com/rs/107-MQW-078/images/yc-1800-brochure.pdf. Accessed December 21, 2023.
6. Mainster MA, Sliney DH, Belcher 3rd CD, Buzney SM. Laser photodisruptors. Damage mechanisms, instrument design and safety. *Ophthalmology*. 1983;90:973−991.
7. Ansys Zemax OpticStudio comprehensive optical design software. Redmond, WA, radiant ZOS LLC. https://www.zemax.com/pages/opticstudio.html. Accessed December 21, 2023.
8. Gu Z, Wang Y, Yan C. Optical system optimization method for as-built performance based on nodal aberration theory. *Opt Express*. 2020;28:7928.
9. Andersen TB. Efficient and robust recurrence relations for the Zernike circle polynomials and their derivatives in Cartesian coordinates. *Opt Express*. 2018;26:18878.
10. *Möller-wedel optical*. Haag-streit Group. Köniz, Switzerland. https://moeller-wedel-optical.com/en/product/measuring-equipment-for-optical-systems-melos-530. Accessed December 21, 2023.
11. Slushetz Y, Patal R, Arieli Y, Mandelbaum YM. yaaqovm/Advanced-Optical-Analysis-of-Divergence-Between-the-Foci-of-the-Nd-YAG-and-Aiming-Beam-Laser: Additional Material. *Zenodo*. 2024. https://doi.org/10.5281/zenodo.10832421.
12. Sharma G, Purkayastha S, Deka H, Bhattacharjee H. Commonly used diagnostic and laser lenses for retinal diseases—an overview. https://www.researchgate.net/publication/327691417_Commonly_Used_Diagnostic_and_Laser_Lenses_for_Retinal_Diseases-An_Overview; 2008. Accessed December 21, 2023.
13. Rol P, Fankhauser F, Kwasniewska S. New contact lens for observation and coagulation of the retina and choroid. *Am J Ophthalmol*. 1988;105(5):479−482.
14. Javitt JC, Tielsch JM, Canner JK, et al. National otcomes of cataract extraction: increased risk of retinal complications associated with Nd:YAG Laser Capsulotomy. *Ophthalmology*. 1992;99:1487−1498.
15. Karahan E, Er D, Kaynak S. An overview of Nd:YAG laser capsulotomy. *Med hypothesis Discov Innov Ophthalmol*. 2014;3:45−50.
16. Sun IT, Lee TH, Chen CH. Rapid cataract progression after Nd:YAG vitreolysis for vitreous floaters: a case report and literature review. *Case Rep Ophthalmol*. 2017;8:321−325.
17. Luo J, An X, Kuang Y. Efficacy and safety of yttrium-aluminium garnet (YAG) laser vitreolysis for vitreous floaters. *J Int Med Res*. 2018;46:4465−4471.

18. Khadka D, Bhandari S, Bajimaya S, et al. Nd:YAG laser hyaloidotomy in the management of premacular subhyaloid hemorrhage. *BMC Ophthalmol*. 2016;16:41.
19. Karagiannis D, Kontadakis GA, Flanagan DND. YAG laser for preretinal hemorrhage in diabetic retinopathy. *Am J Ophthalmol Case Rep*. 2018;10:8–9.
20. Allam K, AlMutairi N, Ellakwa AF, Abdelkader E. Nd:YAG laser therapy for non-resolving premacular subhyaloid hemorrhage in Saudi patients. *Saudi J Ophthalmol*. 2019;33:61–65.
21. Opremcak E, Rehmar AJ, Ridenour CD, et al. Restoration of retinal blood flow via translumenal Nd:YAG embolysis/embolectomy (TYL/E) for central and branch retinal artery occlusion. *Retina*. 2008;28:226–235.
22. Wesolosky JD, Tennant M, Rudnisky CJ. Rate of retinal tear and detachment after neodymium:YAG capsulotomy. *J Cataract Refract Surg*. 2017;43:923–928.
23. Bypareddy R, Chawla R, Azad SV, Takkar B. Iatrogenic parafoveal macular hole following Nd-YAG posterior hyaloidotomy for premacular haemorrhage. *BMJ Case Rep*. 2016;2016:bcr2016217234.
24. Tsai WF, Chen YC, Su CY. Treatment of vitreous floaters with neodymium YAG Laser. *Br J Ophthalmol*. 1993;77:485–488.
25. Delaney YM, Oyinloye A, Benjamin L. Nd:YAG vitreolysis and pars plana vitrectomy: surgical treatment for vitreous floaters. *Eye*. 2002;16:21–26.
26. Shah CP, Heier JS. YAG laser vitreolysis vs sham YAG vitreolysis for symptomatic vitreous floaters: a randomized clinical trial. *JAMA Ophthalmol*. 2017;135:918–923.
27. Su D, Shah CP, Hsu J. Laser vitreolysis for symptomatic floaters is not yet ready for widespread adoption. *Surv Ophthalmol*. 2020;65:589–591.